Maternal GABAergic and GnRH/corazonin pathway modulates egg diapause phenotype of the silkworm *Bombyx mori*

Ryoma Tsuchiya[a], Aino Kaneshima[a], Masakazu Kobayashi[a], Maki Yamazaki[a], Yoko Takasu[b], Hideki Sezutsu[b], Yoshiaki Tanaka[b], Akira Mizoguchi[c], and Kunihiro Shiomi[a,1]

[a]Faculty of Textile Science and Technology, Shinshu University, Ueda 386-8567, Japan; [b]National Agriculture and Food Research Organization, 305-8634 Tsukuba, Japan; and [c]Division of Liberal Arts and Sciences, Aichi Gakuin University, Nisshin 470-0195, Japan

Edited by David Denlinger, The Ohio State University, Columbus, OH, and approved November 23, 2020 (received for review September 24, 2020)

Diapause represents a major developmental switch in insects and is a seasonal adaptation that evolved as a specific subtype of dormancy in most insect species to ensure survival under unfavorable environmental conditions and synchronize populations. However, the hierarchical relationship of the molecular mechanisms involved in the perception of environmental signals to integration in morphological, physiological, behavioral, and reproductive responses remains unclear. In the bivoltine strain of the silkworm *Bombyx mori*, embryonic diapause is induced transgenerationally as a maternal effect. Progeny diapause is determined by the environmental temperature during embryonic development of the mother. Here, we show that the hierarchical pathway consists of a γ-aminobutyric acid (GABA)ergic and corazonin signaling system modulating progeny diapause induction via diapause hormone release, which may be finely tuned by the temperature-dependent expression of plasma membrane GABA transporter. Furthermore, this signaling pathway possesses similar features to the gonadotropin-releasing hormone (GnRH) signaling system for seasonal reproductive plasticity in vertebrates.

diapause hormone | corazonin | GABA | GABA transporter | *Bombyx mori*

To ensure survival under unfavorable environmental conditions and synchronize populations, most insect species enter diapause, which is a seasonal adaptation that evolved as a specific subtype of dormancy (1, 2). Diapause is not a passive response to changing conditions but rather an actively induced state that precedes adverse natural situations. Therefore, this diapause phenotype is accompanied by changes in energy metabolism or storage to improve cold/stress tolerance in later life stages, or progeny via reproductive switch (3). Although it has been generally suggested that brain/neuroendocrine systems are associated with this seasonal reproductive plasticity in both vertebrates and invertebrates (3, 4), the hierarchical relationship of the molecular mechanisms involved in the perception of environmental signals to integration into morphological, physiological, behavioral, and reproductive responses, known as the diapause syndrome, remains unclear (3).

The silkworm *Bombyx mori* is a typical insect that arrests normal development during early embryogenesis, which is accompanied by metabolic changes in diapause (5, 6). The development of diapause-destined embryos is arrested during the G2 cell cycle stage immediately after the formation of the cephalic lobe and telson and sequential segmentation of the mesoderm (7). The bivoltine strain of *B. mori* has two generations per year, and progeny diapause is transgenerationally induced as a maternal effect and is determined by the environmental temperature, photoperiod, and nutrient conditions during embryonic and larval development of the mother (5, 6). The temperature signal during the mother's embryonic development predominantly affects diapause determination, even if silkworms of the bivoltine Kosetsu strain are exposed to all cases of photoperiods during embryonic and larval development. In the Kosetsu strain, when eggs are incubated at 25 °C under continuous darkness, the resultant female moths (25DD) lay diapause eggs in almost all cases. In contrast, incubation of eggs at 15 °C in dark condition results in moths (15DD) that lay nondiapause eggs in almost all cases (6).

Embryonic diapause is induced by the diapause hormone (DH) signaling pathway, which consists of highly sensitive and specific interactions between a neuropeptide, DH, and DH receptor (DHR) (6, 8). DH is exclusively synthesized in seven pairs of neurosecretory cells (DH-PBAN–producing neurosecretory cells [DHPCs]) located within the subesophageal ganglion (SG) in the mother's generation (6). DH is released into the hemolymph during pupal–adult development and acts on the DHR, which belongs to the G protein-coupled receptors (GPCRs) (9). DH levels in the hemolymph are higher in the 25DD than 15DD pupae in the middle of pupal–adult development when the developing ovaries are sensitive to DH (6). Furthermore, the embryonic *Bombyx* TRPA1 ortholog (BmTRPA1) acts as a thermosensitive channel that is activated at temperatures above ∼21 °C and affects diapause induction through DH release (10). However, there remain questions about the thermal information that is received by BmTRPA1 and linked to DH signaling to induce diapause.

Significance

Diapause is a common response to seasonal changes in environmental conditions found in many species of insects, as well as other animals, but we do not yet fully understand the molecular mechanisms underlying this important physiological switch. Although there has been previous research on diapause, there remain questions regarding the molecular mechanisms underlying diapause determination in response to environmental signals. Our research highlighted the presence of a GABAergic and corazonin signaling system that induces progeny diapause through diapause hormone release. Our findings also indicate that the expression of the plasma membrane GABA transporter is temperature-dependent and may modulate diapause hormone release. Our findings provide insights into these mechanisms in silkworms and will provide an important reference for future research.

Author contributions: K.S. designed research; R.T., A.K., M.K., M.Y., Y. Takasu, H.S., Y. Tanaka, A.M., and K.S. performed research; A.M. and K.S. analyzed data; and K.S. wrote the paper.

The authors declare no competing interest.

This article is a PNAS Direct Submission.

[1]To whom correspondence may be addressed. Email: shiomi@shinshu-u.ac.jp.

This article contains supporting information online at https://www.pnas.org/lookup/suppl/doi:10.1073/pnas.2020028118/-/DCSupplemental.

Published December 28, 2020.

From the 1950s, it has been suggested that the DH release was controlled by signals derived from certain region(s) in the brain based on surgical experiments, such as midsagittal bisection or transection (11–13). Especially, the operation in nondiapause producers changed them to diapause producers while transection of the protocerebrum had no effect on the diapause producers. These surgical results suggested the involvement of the protocerebrum in the inhibitory control of DH secretion (12, 14). Furthermore, the accumulation of the ovarian 3-hydroxykynurenine (3-OHK) pigment that accompanies the diapause syndrome was affected by injection with γ-aminobutyric acid (GABA) and the plant alkaloid picrotoxin (PTX), which is a widely used ionotropic GABA and glycine receptor antagonist (15, 16), and the selective ionotropic GABA receptor (GABAR) antagonist bicuculline. This suggests that a GABAergic neurotransmission via ionotropic GABAR is involved in DH secretion, which may be active in nondiapause producers but inactive in diapause producers throughout the pupal–adult development (14, 17). In general, ionotropic GABAR is composed of homo- or hetero-pentameric subunits. All known GABAR subunits display a similar structural scheme, with a large N-terminal extracellular domain involved in the formation of a ligand-binding pocket and a pore domain made of four transmembrane alpha-helices (TM1–TM4) (16, 18). Four homologous sequences of the ionotropic GABAR subunit genes were identified as *RDL*, *LCCH3*, *GRD*, and a GRD-like sequence named *8916* in various insects (19). However, the in vivo physiological roles of both signals derived from the brain and the GABAergic pathway in diapause induction have not been previously investigated.

Corazonin (Crz) is an undecapeptide neurohormone sharing a highly conserved amino acid (a.a.) sequence across insect lineages and is involved in different physiological functions, such as heart contraction (20), stress response (21, 22), various metabolic activities (23–25), female fecundity (26), melanization of locust cuticles (27), regulation of ecdysis (28, 29), and control of caste identity (30). Moreover, Crz belongs to the gonadotropin-releasing hormone (GnRH) superfamily alongside adipokinetic hormone (AKH) and AKH/Crz-related peptide (ACP). Duplicates of an ancestral GnRH/Crz signaling system occurred in a common ancestor of protostomes and deuterostomes through coevolution of the ligand receptor (31, 32).

Herein, we demonstrated that the hierarchical pathway consists of a GABAergic and Crz signaling system modulating progeny diapause induction by acting on DH release. We propose that the PTX-sensitive GABAergic signal may act to chronically suppress Crz release in dorsolateral Crz neurons (under nondiapause conditions) and that diapause conditions (or PTX injection) inhibits GABAergic signaling, resulting in accelerated Crz release, which in turn induces DH release. GABA signaling may be finely tuned by the temperature-dependent expression of the plasma membrane GABA transporter (GAT), which differs between the 25DD and 15DD conditions. Furthermore, this signaling pathway possesses similar features to the GnRH signaling system with respect to seasonal reproductive plasticity in vertebrates.

Results

Ionotropic GABAR Antagonist PTX Acts as a Potent Inducer in Progeny Embryonic Diapause via DH Release. We first verified whether the ionotropic GABAR antagonist PTX, when injected into pupae, induced diapause eggs from both the polyvoltine strain N4, which genetically oviposits nondiapause eggs, and the bivoltine strain Kosetsu (15DD), by in vivo bioassay. This approach is in contrast to previous studies that monitored the accumulation of the ovarian 3-OHK pigment in vitro (14, 17). Nondiapause eggs oviposited from distilled water (DW)-injected silkworms were still yellow and hatched 9 to 10 d after oviposition, as was also the case in noninjected silkworms, but many eggs oviposited from PTX-injected silkworms became brown 2 d after oviposition (Fig. 1 *A* and *B*). These brown eggs never hatched 60 d after oviposition, and normal embryogenesis was arrested immediately after formation of the cephalic lobe and telson and after segmentation of the mesoderm, which is known as the diapausing stage in *B. mori* (6, 33). This was also the case with the eggs from both DH-injected (Fig. 1*B*) and 25DD silkworms (6). However, we could not find other chemicals with respect to the GABAergic pathway, including the GABA affecting the progeny diapause phenotype in the in vivo bioassay (*SI Appendix*, Table S1).

To investigate the mode of action of PTX, we constructed knockout (KO) mutants with respect to *DH-PBAN*, which encodes a polyprotein precursor containing DH, PBAN, and α-, β-, and γ-SGNPs (SG neuropeptides), and *DHR* designated as *ΔDHP* and *ΔDHR*, respectively, in addition to the null mutants *ΔDHP33*, *ΔDHP531*, and *ΔDHR96,* as described previously (6) (*SI Appendix*, Fig. S1 *A–D*). Diapause eggs were induced in a dose-dependent manner in the range of 1.8 to 60 μg per pupa in PTX-injected silkworms of wild type (*wt*) while there were no diapause eggs observed in PTX-injected *ΔDHP13-4* in N4 (Fig. 1*C*). Next, we attempted rescue experiments of KO mutants by coinjecting with synthetic DH to test whether PTX acts in the upstream of the DH signaling pathway in both N4 and Kosetsu (15DD) (Fig. 1 *D* and *E*). In *wt*, PTX had a significant effect on diapause egg-inducing activity at 50 μg per pupa, but no effects were shown in *ΔDHP* mutants; however, coinjection with DH resulted in high diapause egg-inducing activity in both strains (Fig. 1 *D* and *E*). In addition, almost no activity was observed in *ΔDHR96* even after DH injection (Fig. 1*E*).

Next, we analyzed the effects of PTX injection on *DH-PBAN* expression in the brain–SG complex, and DH levels in both the brain–SG complex and hemolymph of PTX-injected pupa during pupal–adult development. No changes in *DH-PBAN* expression were observed following PTX injection during pupal–adult development in N4 and Kosetsu (15DD) (Fig. 1*F* and *SI Appendix*, Fig. S1*E*) whereas the DH content in the brain–SG complex considerably decreased immediately following PTX injection. This was accompanied by increased hemolymph DH concentrations in PTX-injected silkworms (Fig. 1 *G* and *H*, and *SI Appendix*, Fig. S1*F*).

Crz Induction of Egg Diapause Occurs in Hierarchical Upstream of DH Signaling Pathway. We found that injection with synthetic Crz, whose authentic peptide is mainly produced in the dorsolateral region of the brain (34), induced diapause eggs from the nondiapause egg producers N4 and Kosetsu (15DD) (Fig. 2*A*). Diapause egg-inducing activities of Crz in *wt* of both strains were observed in a dose-dependent manner, ranging from 1 pmol to 1 nmol in the tested area, although the efficiency of diapause egg-inducing activity was 1/10 lower than DH. In *DHP* mutants, although Crz could not affect the induction of diapause eggs in both strains, coinjection with Crz and DH rescued the diapause egg-inducing activity, which was similar to that with the DH-only injection (= 50 to 60%) (Fig. 2 *B* and *C*). However, *DHR* KO mutants were not rescued at all by DH injection (Fig. 2*C*).

Next, we tested the effects of Crz injection on *DH-PBAN* expression and DH level in the hemolymph (Fig. 2 *D* and *E* and *SI Appendix*, Fig. S2 *A* and *B*). No significant differences were observed in *DH-PBAN* expression during the pupal–adult development whereas DH titers were considerably increased at 6 h (i.e., 1.25 d after pupation [P1.25]) after Crz injection in both strains.

To investigate whether endogenous Crz functions in diapause induction, we constructed KO mutants for both Crz and a GPCR (BNGR-A21) known as the Crz receptor (CrzR) (35). We successfully isolated the KO mutant of *CrzR*, *ΔCrzR515*, as well as a mutant of *Crz* in the Kosetsu strain that inserted three

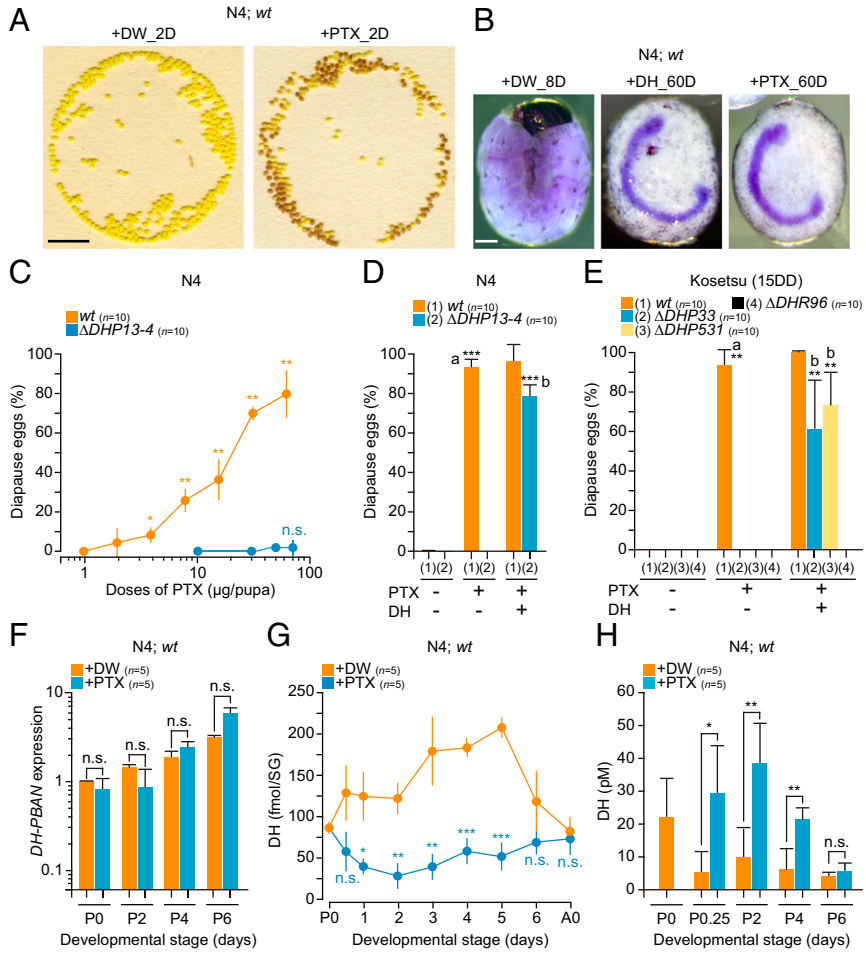

Fig. 1. Ionotropic GABAR antagonist plant alkaloid PTX acts as a potent inducer in progeny diapause via DH release. (*A*) The typical egg batches oviposited from each DW-injected (+DW_2D) and PTX-injected (+PTX_2D) silkworm of *wt* in N4 strain. Representative images of eggs 2 d after oviposition. (Scale bar: 1 cm.) (*B*) Thionin staining of embryos 8 d after oviposition in DW-injected silkworms (+DW_8D), and 60 d after oviposition in DH-injected (+DH_60D) and PTX-injected (+PTX_60D) silkworms in *wt* of N4 strain. (Scale bar: 200 μm.) (*C*) Dose–response curves of PTX on diapause egg-inducing activity. The PTX was injected into *wt* and KO mutant of *DH-PBAN* (*ΔDHP13-4*) in N4. Each bar represents the mean ± SD of 10 animals. The significant differences represented against the activity at 0.94 μg per pupa dose in *wt*. (*D* and *E*) Rescue experiments by injection of DH in KO mutants of *DH-PBAN* (*ΔDHP13-4*, *ΔDHP33*, and *ΔDHP531*) and *DHR* (*ΔDHR96*). Pupae were injected with 50 μg of PTX (+) or not (–) 1 d after pupation; thereafter, pupae were injected with 100 pmol DH (+) or not 3 d after pupation in N4 (*D*) and Kosetsu (*E*), and the diapause egg-inducing activity was measured. Each bar represents the mean ± SD of 10 animals. The significant differences vs. *wt* (PTX –, DH –; a) or *ΔDHP* (PTX +, DH –; b) are represented. (*F*) Effect of PTX injection on *DH-PBAN* expression in brain–SG complex during pupal–adult development. The PTX or DW was injected just after pupation (+PTX or +DW); thereafter, the brain–SG complex was dissected out. Each bar represents the mean ± SD of five samples. (*G*) Effect of PTX injection on DH content in brain–SG complex during pupal–adult development. Each bar represents the mean ± SD of five animals. (*H*) Effect of PTX injection on DH titer in hemolymph during pupal–adult development. PTX was injected just after pupation (P0). +DW and +PTX represent DW and PTX injections, respectively. Each bar represents the mean ± SD of five samples. n.s., nonsignificant; $*P < 0.05$; $**P < 0.01$; $***P < 0.001$.

nucleotides coding aspartic acid (D) between positions 7 and 8 from the N terminus and named it as *Crz/7_8insD* (Fig. 2*F* and *SI Appendix*, Fig. S2 *C–F*). Using the chemically synthesized Crz/7_8insD, the diapause-inducing activity was tested in N4 (*wt*) and Kosetsu (15DD) (Fig. 2*A*). No activities were observed even at the 10-nmol dose in both strains. When the *Crz/7_8insD* mutant was incubated under 25DD conditions, diapause eggs were oviposited at a proportion of ∼40% (Fig. 2*F*, bar W). The *Crz7_8insD* pupated over 2 d, and the egg batches were divided into two populations: The egg batches oviposited from moths that pupated on the first day were named the early (E) population, and the egg batches from moths that pupated on the next day were named the late (L) population. Interestingly, almost all nondiapause eggs oviposited in E. In addition, DH titers of the early population silkworms significantly decreased during the pupal stage, similar to *wt* (15DD) (Fig. 2*G*). In addition, no changes were observed in the diapause-inducing activity in the *CrzR* KO mutant in 25DD (Fig. 2*F*).

Putative GABAR Subunit *8916* Ortholog Expresses in Crz Neurons and Participates in Progeny Diapause Induction. Since the diapause-inducing activity in *Crz/7_8insD* was rescued by PTX injection as well as Crz and DH injection, there were two possibilities in the hierarchical relationship: 1) the Crz signal acts in the upstream of the GABAergic pathway, or 2) other factors and receptors cooperatively act with Crz in the downstream of the PTX-sensitive GABAergic pathway (Fig. 2*F*). Hence, we next investigated the hierarchical relationship between the GABAergic pathway and Crz activity. Firstly, we tested whether the PTX injection affected *Crz* expression (*SI Appendix*, Fig. S3*A*). In both N4 and Kosetsu (15DD), there was no difference in expression between DW- and PTX-injected pupae during PTX-sensitive stages

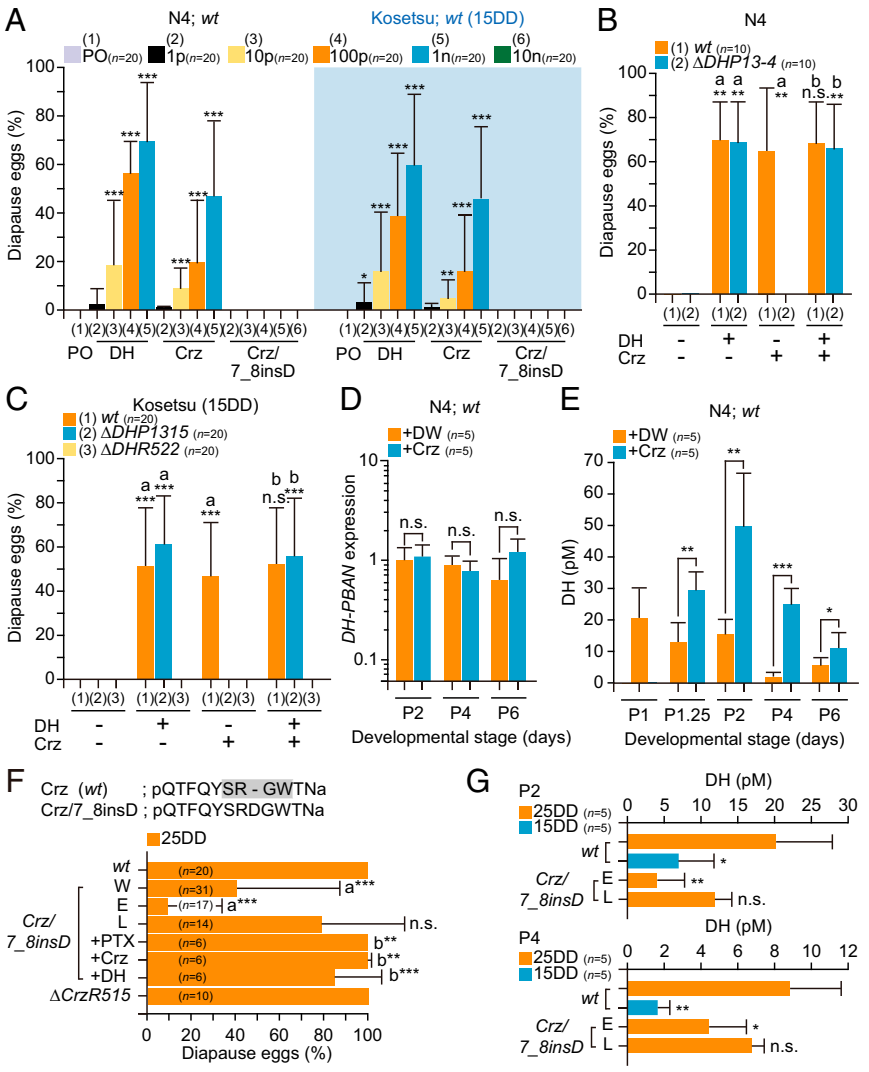

Fig. 2. Crz induces egg diapause at the hierarchical upper level in the DH signaling pathway. (*A*) Diapause egg-inducing activity of each DH, Crz, and Crz/7_8insD injection. The peanut oil (PO) or each peptide (1, 10, 100 pmol, or 1 nmol), and 10 nmol Crz/7_8insD was injected into *wt* pupa in both N4 and Kosetsu (15DD), and the diapause egg-inducing activity was measured. Each bar represents the mean ± SD of 20 animals. Asterisks indicate significant differences vs. PO injection of each strain. (*B* and *C*) Rescue experiments by injection of DH in KO mutants of *DH-PBAN* (*ΔDHP13-4*, *ΔDHP1315*) and *DHR* (*ΔDHR522*). Pupae were injected with Crz (1 nmol) (+) or not (–) 1 d after pupation; thereafter, pupae were injected with DH (100 pmol) (+) or not (–) 3 d after pupation in N4 (*B*) and Kosetsu (*C*), and the diapause egg-inducing activity was measured. Each bar represents the mean ± SD of 10 to 20 animals. The significant differences vs. (DH –, Crz –; a) or (DH –, Crz +; b) are represented. (*D*) Effect of Crz injection on *DH-PBAN* expression in brain–SG complex during pupal–adult development. Crz was injected 1 d after pupation; thereafter, the brain–SG complex was dissected out. Each bar represents the mean ± SD of five samples. (*E*) Effect of Crz injection on DH titer in hemolymph during pupal–adult development. Crz (1 nmol) and DW were injected 1 d after pupation (P1). +DW and +Crz represent the DW and Crz injection, respectively. Each bar represents the mean ± SD of five samples. (*F*) The a.a. sequences of Crz in *wt* and Crz/7_8insD. The –SXGW– conserved sequence of Crz is indicated by the gray box. Diapause egg-inducing activity in both mutants of *Crz* and *CrzR*, *Crz/7_8insD* and *ΔCrzR515* in 25DD. The proportions of diapause eggs oviposited from *wt* (*wt*) and KO mutant (–) female moths were measured as well as that of injected moth; each plant alkaloid PTX, Crz, and DH was injected at 50 μg, 1 nmol, and 100 pmol per pupa, respectively. In *Crz/7_8insD*, whole egg batches (W) were divided into two populations: early (*E*) and late (L). The significant differences vs. *wt* or E are represented at a or b, respectively. (*G*) DH levels in hemolymph 2 (P2) or 4 (P4) d after pupation in *Crz/7_8insD*. Each bar represents the mean ± SD of five samples. The significant differences vs. *wt* (25DD) are represented. n.s., non-significant; **P* < 0.05; ***P* < 0.01; ****P* < 0.001.

P0 and P2. However, the immunoreactivity of Crz was considerably decreased in PTX-injected pupae 3 d later (Fig. 3 *A*–*C*). The immunoreactivity of Crz was clearly detected in the dorsolateral region in DW-injected pupae, which have been known as Crz neurons in the protocerebrum (34) (Fig. 3 *A* and *B*, +DW). The signal intensity of PTX-injected pupae decreased in the somata and arbitrarily limited areas of the axons at 50% and 20%, respectively, compared with DW-injected pupae (Fig. 3 *B* and *C* and *SI Appendix*, Fig. S3*B*). Therefore, we assumed that not only the dorsolateral Crz neurons were the target cells expressing the PTX-sensitive inotropic GABAR subunits but also that PTX could act on Crz neurons to release Crz.

In *B. mori*, five orthologs of GABAR subunit genes were identified and named as *BmRDL1*, *RDL2*, *RDL3*, *LCCH3*, and *GRD* (36). However, we proposed changing the nomenclature of "*BmGRD*" to "*Bm8916*" since the *BmGRD* ortholog exhibits a close sequence relationship with other *8916* but not *GRD* as reported previously (Fig. 3*D*) (37, 38). We tried cloning and sequencing each subunit gene in both N4 and Kosetsu strains, resulting in the *RDL1*, *RDL2*, *RDL3*, *LCCH3*, and *8916* orthologs

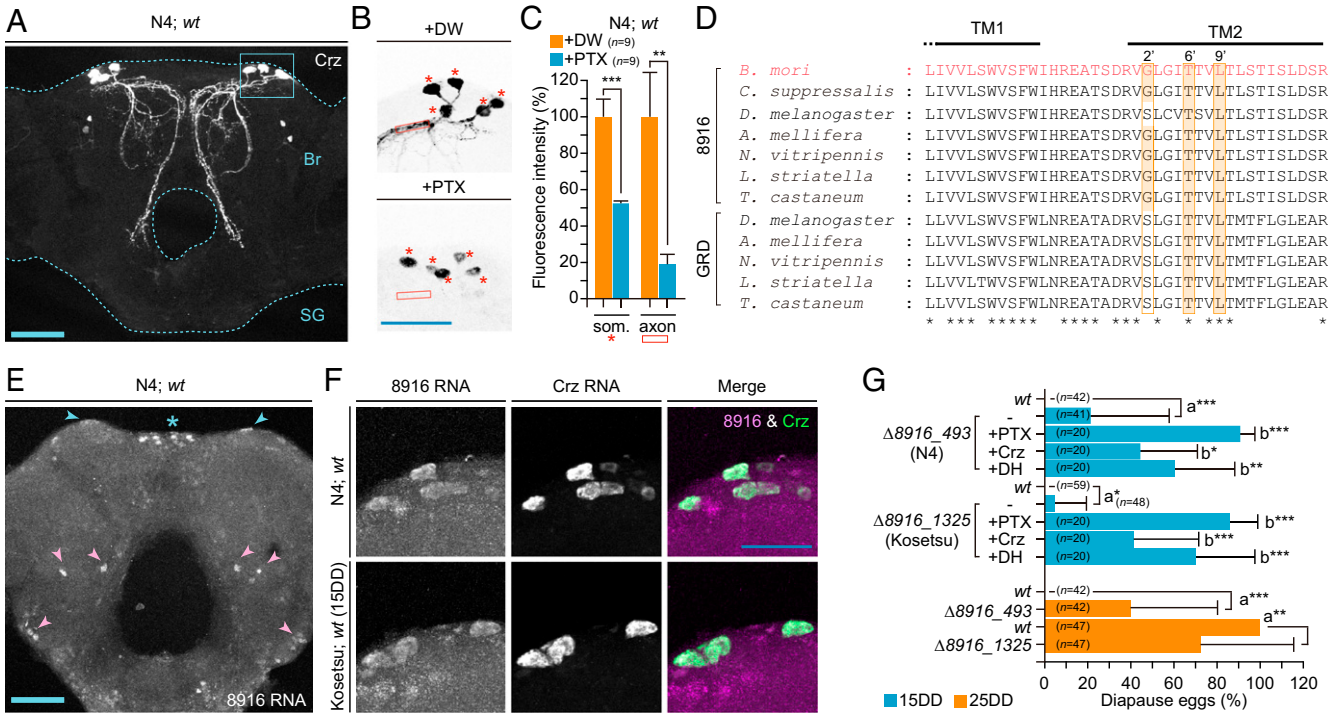

Fig. 3. Putative GABAR subunit gene *8916* ortholog expresses in Crz neurons and participates in progeny diapause determination. (*A*) Immunostaining of Crz neurons in pupal brain-SG complex (dotted lines). The box indicates the Crz neurons in the dorsolateral region of the brain (Br). (*B*) The plant alkaloid PTX-injection affected the intensity of Crz immunoreactivity in dorsolateral Crz neurons. PTX (50 μg) or DW was injected into pupae just after pupation. The brain–SG complex was dissected out 3 d after injection, and immunostaining was performed. Images of immunostaining in brain from DW-injected (+DW) and PTX-injected (+PTX) pupae are represented. The arbitrarily limited areas of the somata and axons are indicated by asterisks and the box, respectively. (*C*) The relative fluorescence intensity in the dorsolateral Crz neurons is shown as a percentage of that of +DW. Each bar represents the mean value of nine samples ± SD. (*D*) Sequence alignment between TM1 and TM2 of 8916 and GRD subunit orthologs among the insects. GenBank accession numbers are as follows: 8916 of *B. mori* (AB278157), *Chilo suppressalis* (KX856967), *D. melanogaster* (NP_001162770.1), *A. mellifera* (DQ667193), *Nasonia vitripennis* (FJ851093.1), *Laodelphax striatella* (KX355314.1), and *Tribolium castaneum* (EF545127.1), GRD of *D. melanogaster* (CAA55144.1), *A. mellifera* (AJE68942.1), *N. vitripennis* (XP_008206161.1), *L. striatella* (AOO87783.1), and *T. castaneum* (NP_001107772.1). Orange boxes at 2′, 6′, and 9′ positions of TM2 residues in each subunit implicated in PTX binding. *, a.a. corresponding among 8916 and GRD. (*E*) RNAscope detection of *8916* RNA in whole brain of N4. The positive signals were detected in dorsolateral regions (blue arrowheads), midline (*), and others (pink arrowheads) of brain. (*F*) Colocalization of *8916* and *Crz* RNA in Crz neurons of brain in N4 and Kosetsu (15DD). RNA signals of *8916* (magenta) and *Crz* (green) were merged by using the RNAscope probes. (*G*) Diapause egg-inducing activity in KO mutants of *8916*, *Δ8916_493*, and *Δ8916_1325* of N4 and Kosetsu. The proportions of diapause eggs oviposited from *wt* (*wt*) and KO mutant (–) female moths were measured as well as that of moths injected with PTX, Crz, and DH at 50 μg, 1 nmol, and 100 pmol per pupa, respectively. The significant differences vs. *wt* (a), or (–) (b) are represented. n.s., nonsignificant; $*P < 0.05$; $**P < 0.01$; $***P < 0.001$. (Scale bars: 100 μm.)

being determined (*SI Appendix*, Fig. S3*C*), but we could not find the *GRD* ortholog in genome databases like other Lepidoptera (38). We performed the expression analysis using RT-PCR (*SI Appendix*, Fig. S3*D*). Each subunit was expressed during embryonic and postembryonic development, with especially high expression being observed in the larval and pupal brain–SG complex.

Based on the hypothesis outlined above, we attempted screening by in situ hybridization using RNAscope technology to identify the GABAR subunits expressed in dorsolateral Crz neurons. Using the *8916* probe, we observed that positive signals were localized in the whole brain, including in the pars intercerebralis and dorsolateral cells, and no signals were observed in DHPCs (Fig. 3*E*). With double staining using probes *8916* and *Crz*, fluorescence signals corresponded in dorsolateral Crz neurons (Fig. 3*F*). Therefore, we speculated that the *8916* subunit is a candidate comprising the ionotropic GABAR complex, which participated with DH release in the hierarchical upstream of Crz signaling.

Next, we investigated whether the *8916* KO silkworms oviposited diapause eggs from nondiapause egg producers N4 and Kosetsu (15DD) (*SI Appendix*, Fig. S4 *A* and *B*). Under the 15DD condition, although the moths of both strains laid all nondiapause eggs in *wt*, the *8916* KO mutants, *Δ8916_493* in N4 and *Δ8916_1325* in Kosetsu, laid slightly but significantly more diapause eggs (493, $P = 0.0003$; 1,325, $P = 0.0331$) (Fig. 3*G*). Furthermore, when each of PTX, Crz, and DH was injected into these mutants, higher diapause egg-inducing activity was observed. However, there were no significant differences in DH titers observed between *wt* and KO mutants (*SI Appendix*, Fig. S4 *C* and *D*). Interestingly, more diapause eggs were oviposited under the 25DD condition of N4 and Kosetsu (Fig. 3*G*), suggesting that not only the *8916* subunit participated in the suppression of the Crz and DH signaling pathway but also *Δ8916* disrupted progeny diapause even under the 25DD condition.

High Expression of Plasma Membrane *GAT* Ortholog under 25DD Is Involved in Diapause Determination. GABA neurotransmission requires a specialized set of proteins to synthesize, transport, or respond to GABA in the nervous systems of both vertebrates and invertebrates (39, 40). In 25DD and 15DD female pupae of the Kosetsu strain, there may be neuroendocrine plasticity in the GABAergic/Crz pathway in conjunction with reception of the different temperature conditions during the embryonic development. To reveal this point, we performed cloning and quantitative PCR analysis of 10 classified genes involved in GABAergic neurotransmission (40) (Fig. 4*A*) in the brain–SG complex during pupal–adult development. We successfully identified each of the 10 classified genes by searching KAIKObase (https://sgp.dna.affrc.

go.jp/KAIKObase/). No differences were observed in gene expression between 25DD and 15DD pupae on nine genes, including *8916* (*SI Appendix*, Fig. S5*A*). However, we found that the expression of the plasma membrane *GAT* ortholog was 10- to 100-fold more highly expressed in the brain–SG complex of 25DD throughout pupal–adult development compared with that in 15DD (Fig. 4*B*). Therefore, we generated two KO mutants for *GAT*, *ΔGAT292*, and *ΔGAT3225* (*SI Appendix*, Fig. S4 *B* and *C*) to observe the progeny diapause phenotype and DH levels in the hemolymph. Under 25DD conditions, the female adults of each KO mutant oviposited mostly nondiapause eggs with ∼20% diapause eggs (Fig. 4*C*). Furthermore, injection with PTX, Crz, and DH rescued the diapause phenotype. Moreover, DH levels in the 25DD condition of each KO mutant were low compared with 25DD and similar to 15DD in *wt* in both the P2 and P4 during the pupal–adult development (Fig. 4*D*), and especially significant differences appeared in the P4 stage. Two mutants oviposited nondiapause eggs in 15DD silkworms, as well as in *wt* (*SI Appendix*, Fig. S5*D*). In addition, injection with PTX, Crz, and DH resulted in the oviposition of diapause eggs.

Discussion

Our results suggest that, under nondiapause conditions, the PTX-sensitive GABAergic signal may act to suppress Crz release in dorsolateral Crz neurons, which in turn suppresses DH release and thereby inhibits the formation of diapause eggs. For more than half a century, the molecular and neural pathways regulating DH release have remained unclear, despite the many studies on this topic. Several works have outlined various hypotheses regarding the signals derived from particular areas of the cerebrum, which have stimulating or inhibiting actions (14). Consistent with these hypotheses, we report results that identify the cerebral cells in which Crz neurons contribute to DH release. In *Drosophila*, the Crz neurons have axon terminations impinging on insulin-producing cells (41), and Crz neurons are also connected to prothoracicotropic hormone neurons and prothoracic gland cells (29), resulting in Crz regulating stress resistance, metabolism, and systemic growth. Moreover, *Bombyx* Crz neurons projected into the corpus cardiacum (CC), a major release site for neuropeptide hormones including the DH, from which Crz may be released into the hemolymph (34). In addition, the axons with bead-like varicosities of Crz neurons were localized adjacent to the axons of DHPCs in the CC (*SI Appendix*, Fig. S5*E*). Therefore, it is possible that the Crz neurons are directly or indirectly connected to DHPCs and/or the CC so that Crz may act as a local neuromodulator/cotransmitter or neurohormone.

Reproduction in vertebrates is primarily regulated by the hypothalamic–pituitary–gonadal (HPG) axis. GnRH released from the hypothalamus induces the secretion of gonadotropins from the pituitary, which activates gonadal function and triggers

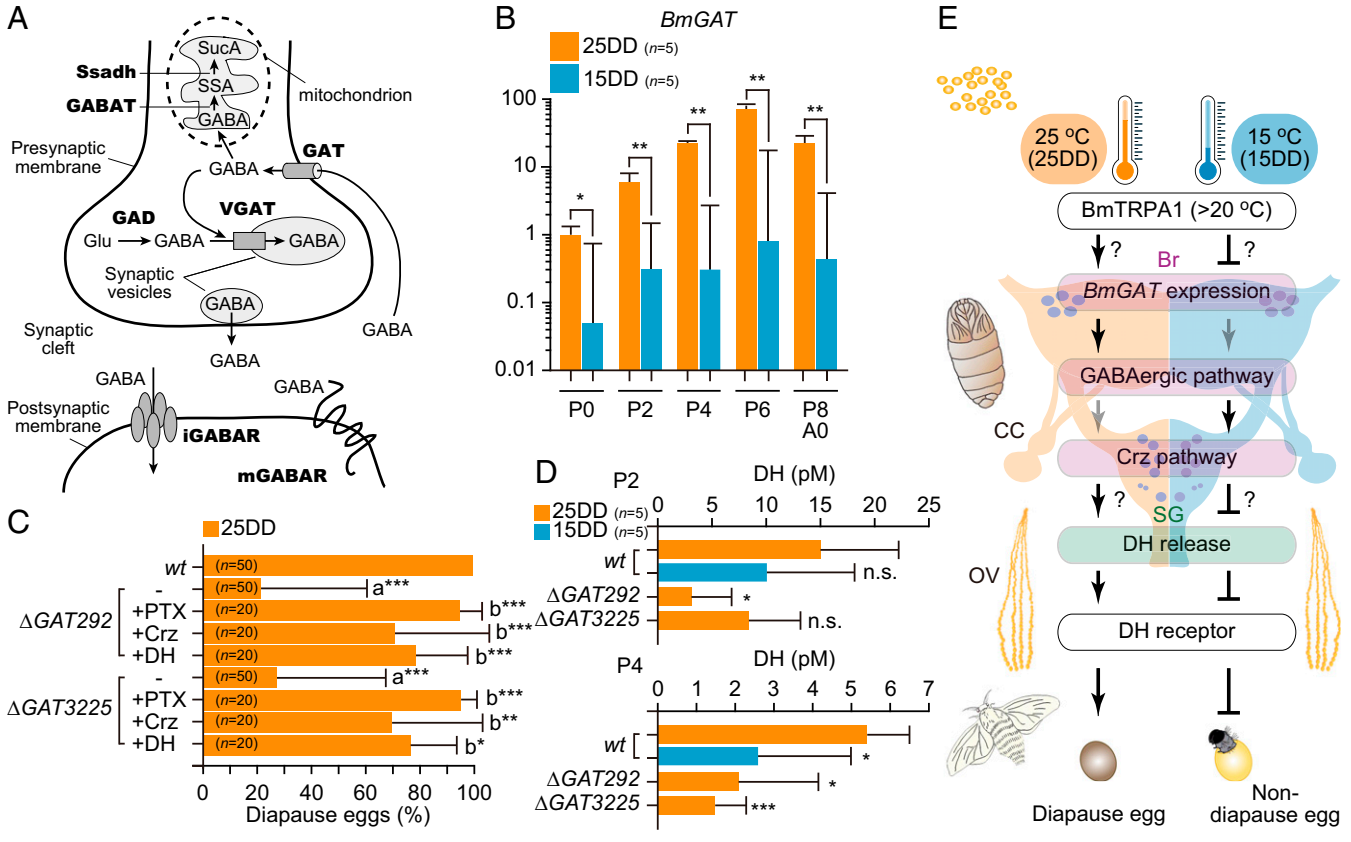

Fig. 4. High expression of the plasma membrane *GAT* in 25DD is involved in diapause determination. (*A*) Schematic overview of a GABAergic synapse cited from Ilg et al. (40). SucA, succinic acid; SSA, succinic semialdehyde; Ssadh, succinic semialdehyde dehydrogenase; GABAT, GABA transaminase; GAT, plasma membrane GABA transporter; VGAT, vesicular GABA transporter; Glu, L-glutamate; GAD, glutamate decarboxylase; iGABAR, ionotropic GABAR; mGABAR, metabotropic GABAR. (*B*) Relative *GAT* mRNA levels in the brain–SG complex between 25DD and 15DD in *wt* during pupal–adult development. The brain–SG complexes were collected every other day just after pupation (P0). Each bar represents the mean ± SD of five sample pupae. (*C*) The diapause egg-inducing activity in KO mutants of *GAT*, *ΔGAT292*, and *ΔGAT3225*. The proportions of diapause eggs oviposited from *wt* (*wt*) and KO mutant (–) female moths of 25DD were measured as well as that of moths injected with plant alkaloid PTX, Crz, and DH at 50 μg, 1 nmol, and 100 pmol per pupa, respectively. The significant differences vs. *wt* (a) or (–) (b) are represented. (*D*) DH levels in hemolymph 2 (P2) and 4 (P4) d after pupation in both *wt* and KO mutants of *GAT*. The significant differences vs. *wt* (25DD) are represented. n.s., nonsignificant; $*P < 0.05$; $**P < 0.01$; $***P < 0.001$. (*E*) Schematic representation of the putative hierarchical pathway in diapause induction. The details are described in *Discussion*.

reproductive activity (42, 43). For seasonal breeders, activation of the HPG axis, including control of GnRH secretion, results in a considerable change in gonadal size, particularly in birds, in which it increases more than a 100-fold during the breeding season in response to seasonal changes, such as in photoperiod (42, 43). Not only Crz structurally belongs to the GnRH superfamily, but SG/CC is also functionally comparable to the vertebrate pituitary gland (44). Indeed, we previously demonstrated that the bicoid-like homeobox gene *Pitx1* (pituitary homeobox 1) ortholog binds to the *cis*-regulatory element of *DH-PBAN* and activates *DH-PBAN* expression (45). Mammalian Pitx1 is present in all pituitary lineages and is a strong activator of several pituitary-specific promoters, including the gonadotropins, luteinizing hormone β-subunit, and follicle-stimulating hormone (46). Although the common ancestor of the GnRH/Crz signaling system ultimately gave rise to the paralogous GnRH-type and Crz signaling systems through ligand receptor coevolution, there are analogous neuroendocrine systems with respect to the seasonal reproductive plasticity between *B. mori* and vertebrates.

In previous reports, it was shown that synthetic Crz, but not AKH, acts to reduce both the spinning rate and the rate of increase in hemolymph ecdysteroid level in *B. mori* (47, 48), suggesting that Crz has multiple physiological functions via the spaciotemporal regulation of ligand–receptor interactions in the Crz signaling system. Using in vitro assay, it was shown that Crz activated CrzR but did not cross-react with AKHR and ACPRs. Conversely, AKHs did not activate CrzR. Therefore, it has been proposed that both AKH and ACP receptors are distinct from the Crz/CrzR signaling system and should rather be grouped into each AKH/AKHR and ACP/ACPR signaling system (35, 49). However, Crz may act cooperatively with AKH/ACP peptides in DH release. None of the synthetic Crz/7_8insD peptides that disrupted the –SXGW– conserved sequence of GnRH/Crz exhibit diapause-inducing activity (32). However, there was no complete loss of diapause-inducing activity in the mutant line *Crz/7_8insD*. Moreover, the KO mutant of CrzR, *ΔCrzR515*, was not affected in diapause induction. Taken together, we speculated that not only Crz interacts with other GPCR in vivo but also other related peptides cooperatively act with Crz in DH release. In addition, batches of nondiapause eggs were observed more frequently in the earlier-pupated moths than those that pupated later in *Crz/7_8insD*, suggesting that the unknown factors controlling growth and metamorphosis may affect both Crz and related peptide actions. Incidentally, not only the *Crz/7_8insD* silkworms were fully viable, and we could not observe abnormalities in growth and development, but also the –SXGW– sequence was shown to be nonessential for eliciting Crz activity (48), indicating that *Crz/7_8insD* was a hypomorphic mutant.

In vertebrates, GnRH neurons express both ionotropic $GABA_A$ and metabotropic $GABA_B$ receptors and receive GABAergic inputs, which is implicated as a major player in the regulation of GnRH neuron activity and secretion (50). Similarly, our results indicated that Crz neurons expressed ionotropic GABAR subunit *8916*, which may receive and input the GABAergic signal. Ionotropic GABARs belong to the Cys-loop ligand-gated ion channel (LGIC) superfamily and play an important role in both inhibitory and excitatory conductance in the nervous systems of both vertebrates and invertebrates, and thus function in multiple physiological situations (18, 19). In addition, with mutagenesis, electrophysiology and structural analyses have shown that the 2′ (Ala), 6′ (Thr), and 9′ (Leu) of TM2 residues in each subunit are implicated in PTX binding (16, 51–53). In insects, homomeric *Apis mellifera* RDL and *Drosophila melanogaster* RDL form PTX-sensitive functional GABAR, as well as heteromeric combinations *Am*RDL/LCCH3, *Am*RDL/GRD, and *Am*GRD/LCCH3, and *Dm*GRD/LCCH3 (18, 54). By contrast, heteromeric *Dm*RDL/LCCH3 was PTX insensitive (18). Furthermore, each *Am* and *Dm*GRD/LCCH3 is a nonspecific cationic channel (54, 55). Thus, ionotropic GABARs can form homo- or heteropentameric complexes with different distinct subunits so that each GABAR has different antagonist sensitivity and ion selectivity (18). Amino acid sequence alignment of the *B. mori* ionotropic GABAR subunit orthologs showed that all subunits exhibited not only features common to members of the LGIC superfamily (36) but also conserved PTX-binding motifs similar to those found in insects and other arthropods (*SI Appendix*, Fig. S3 *C* and *E*), but the amino acid at 2′ was not conserved. To our knowledge, functional analysis of 8916 has never previously been carried out. We speculated that the 8916 subunit comprised the PTX-sensitive GABAR, which may not only form the heteromeric complex with another GABAR subunit but also another subunit that compensated the 8916 function since the effect of the KO mutant of 8916 was lower in diapause induction. We could not test the electrophysiological properties of GABAR carrying 8916 in the present study. Therefore, we could not conclude whether the GABAR subunits composed of 8916 function as PTX-sensitive GABARs.

We identified plasma membrane GAT as a key factor in diapause determination. The plasma membrane GAT belongs to a family of neurotransmitter/sodium symporters that, in humans, is referred to as the solute carrier 6 family (56). GAT actively transports GABA from the synaptic cleft back into presynaptic neurons and glial cells to terminate GABA-stimulated responses (Fig. 4*A*). As a result, these transporters play a pivotal role in maintaining the fidelity of neurotransmission by regulating both the concentration and duration of GABA within the synaptic cleft (56). The *Bombyx* ortholog of the GAT contains highly homologous amino acid sequences against *Manduca sexta* GAT, which is similar to the mammalian GAT-1 in terms of pharmacological properties (57, 58). Therefore, *Bombyx* GAT may function as transporters and may have the ability to induce plastic changes in the strength of GABAergic signals and the activity of neuronal networks in the brain through temperature-dependent expression between the 25DD and 15DD conditions.

In Fig. 4*E*, we summarize the putative molecular hierarchical relationship in progeny diapause induction in *B. mori*. To complete the diapause determination, embryonic thermal information is stored for a long period (~1 mo) until the middle pupal–adult development when it is finally transduced to the neuroendocrine DH signaling pathway. In 25DD, BmTRPA1 is activated at temperatures above ~21 °C and affects diapause induction through the DH signaling pathway (6, 10). During pupal–adult development, high pupal *GAT* expression is induced in the brain–SG complex so that the rapid clearance of GABAergic signals may not suppress Crz release, which accelerates DH release into the hemolymph. When eggs were incubated under 15DD conditions, no activation of BmTRPA1 may suppress *GAT* expression so that prolonged GABAergic signals may act constantly on Crz neurons to suppress Crz release from the somata, and thereafter the suppression of DH release occurs. Thus, GAT may finely tune the hierarchical pathway to determine diapause phenotype through gene expression. In KO mutants of *GAT*, GABA spillover may disrupt the maintenance of normal GABAergic activity and act in DH release, but the molecular mechanisms remain unclear as does the pathway from TRPA1 activation to GAT expression through putative epigenetic control. This seasonal reproductive plasticity conforms to the phenomenon known as a predictive adaptive response and is matched to the environment predicted to be experienced at a later phase in the organism's life history, or by progeny more distant than the next generation (59, 60). Our findings provide knowledge on the molecular hierarchical relationship underlying diapause determination in silkworms and furthers our understanding of predictive adaptive response as a model.

Materials and Methods

Silkworms. The polyvoltine (N4), univoltine (Ascoli-koken), and bivoltine (Kosetsu) strains were used in these experiments. The N4 and Ascoli-koken genetically oviposited nondiapause and diapause eggs, respectively. These eggs were usually incubated at 25 °C under continuous illumination except for the KO mutant of *8916*, *Δ8916_493* of N4 shown in Fig. 3*G*. Eggs of the Kosetsu strain were incubated under two different conditions: 1) at 25 °C under continuous darkness (25DD) to obtain diapause eggs in the *wt*, and 2) at 15 °C under continuous darkness (15DD) to obtain nondiapause eggs in the *wt*. Detailed methods are provided in *SI Appendix, Materials and Methods*.

Injection of Chemicals and Peptides. Each chemical was dissolved with DW and injected into pupae through the intersegmental membrane between the second and third abdominal segments with 20 μL 1 to 6 h after pupation. Each peptide was dissolved in peanut oil (Sigma Aldrich), and 10-μL solutions of various doses were injected into pupae. Detailed methods are provided in *SI Appendix, Materials and Methods*.

Transcription Activator-Like Effector Nuclease and CRISPR-Cas9 Systems. The transcription activator-like effector nuclease (TALEN)-based mutant lines were constructed according to Takasu et al. (61) and Shiomi et al. (6) with some modifications. Detailed methods are provided in *SI Appendix, Materials and Methods*. In the CRISPR-Cas9 system, CRISPR RNA (crRNA) containing a target sequence was designed using CRISPR direct (https://crispr.dbcls.jp/) and purchased as Alt-R CRISPR-Cas9 crRNA from IDT (Coralville, IA). Both Alt-R CRISPR-Cas9 trans-activating crRNA (tracrRNA) and Alt-R Cas9 enzyme were also purchased from IDT. The ribonucleoprotein complex was prepared according to the Alt-R CRISPR-Cas9 system.

DH Levels in Brain–SG Complex and Hemolymph. The DH extract was prepared from the brain–SG complex and hemolymph according to Kitagawa et al. (62) and Shiomi et al. (6), respectively. Detailed methods are provided in *SI Appendix, Materials and Methods*.

Complementary DNA Cloning. We obtained the ortholog sequences of 10 complementary DNAs (cDNAs) with respect to the GABAergic neurotransmission, ionotropic GABAR subunits (*RDL1*, *RDL2*, *RDL3*, *LCCH3*, and *8916*), cytosolic glutamate decarboxylase (GAD), vesicular GABA transporter (VGAT), plasma membrane GAT, mitochondrial GABA-degradative enzymes GABA transaminase (GABAT), and succinic semialdehyde dehydrogenase (Ssadh) (Fig. 4*A*) by searching KAIKOBLAST (kaikoblast.dna.affrc.go.jp/). Detailed methods are provided in *SI Appendix, Materials and Methods*.

RT-PCR and qPCR Analysis. For RT-PCR analysis, poly $(A)^+$ RNAs and first-strand DNA were prepared according to Shiomi et al. (63). Detailed methods are provided in *SI Appendix, Materials and Methods*. In the qPCR, the five brain–SG complexes were collected into one tube as one composite sample. Detailed methods are provided in *SI Appendix, Materials and Methods*.

Thionin Staining, Immunostaining, and RNAscope. Thionin staining was performed as previously described (6). Detailed methods are provided in *SI Appendix, Materials and Methods*. For immunostaining, we generated and used the affinity purified anti-Crz guinea pig antibody against the synthetic Crz conjugated to bovine serum albumin (BSA) with Cys at the C terminus. The anti-DH[N] antibody was used as previously described (13). Detailed methods are provided in *SI Appendix, Materials and Methods*. To determine the relative fluorescence intensity of the dorsolateral Crz-producing somata and its axon, we compared the intensity of the mean pixel fluorescence for individual somata and its axon. Detailed methods are provided in *SI Appendix, Materials and Methods*. We performed the in situ hybridization using an RNAscope Fluorescent Multiplex Reagent kit (Advanced Cell Diagnostics [ACD], Inc., Newark, CA). The probes were designed and prepared by ACD. We developed the method adapting for whole-mount in situ hybridization in the *Bombyx* brain–SG complex. Detailed methods are provided in *SI Appendix, Materials and Methods*.

Statistical Analysis. Statistical parameters, including definitions and exact values of *n*, are provided in the relevant figures or corresponding figure legends. Statistical analyses were performed in Excel 2011 (Microsoft) with the software add-in Toukei–Kaiseki Ver. 3.0 (Esumi). The significance of differences presented in diapause egg-inducing activity was evaluated using the Steel–Dwass test. Other data were compared using Student's *t* tests. Data were expressed as the mean ± SD. $P < 0.05$ was considered to be significant; n.s., nonsignificant; $*P < 0.05$; $**P < 0.01$; $***P < 0.001$.

Data Availability. All study data are included in the article and *SI Appendix*.

ACKNOWLEDGMENTS. We thank Mrs. T. Ikeda and K. Ohishi for silkworm rearing. The RNAscope technique was supported by Dr. A. Mochizuki (Advanced Cell Diagnostics, Inc.). We also thank Dr. K. Yazawa and Mr. A. Murata for useful discussion on the statistical analysis. This research was funded by grants-in-aid from the Ministry of Education, Science, Sports and Culture of Japan, and was supported partly by the Teimei Empress's Memorial Grant of The Dainippon Silk Foundation and the NAITO Foundation. We are also indebted to the Division of Gene Research, Research Center for Human and Environmental Sciences for providing facilities for these studies. We thank Editage for English language editing.

1. V. Kostál, Eco-physiological phases of insect diapause. *J. Insect Physiol.* **52**, 113–127 (2006).
2. D. A. Hahn, D. L. Denlinger, Energetics of insect diapause. *Annu. Rev. Entomol.* **56**, 103–121 (2011).
3. D. L. Denlinger, G. D. Yocum, J. P. Rinehart, "Hormonal control of diapause" in *Insect Endocrinology*, L. I. Gilbert, Ed. (Academic Press, San Diego, 2012), pp. 430–463.
4. L. M. Garcia-Segura, *Hormones and Brain Plasticity* (Oxford University Press, 2009).
5. O. Yamashita, K. Hasegawa, "Embryonic diapause" in *Comprehensive Insect Physiology, Biochemistry and Pharmacology*, G. A. Kerkut, L. I. Gilbert, Eds. (Pergamon Press, Oxford, 1985), vol. 1, pp. 407–434.
6. K. Shiomi *et al*., Disruption of diapause induction by TALEN-based gene mutagenesis in relation to a unique neuropeptide signaling pathway in Bombyx. *Sci. Rep.* **5**, 15566 (2015).
7. M. Nakagaki, R. Takei, E. Nagashima, T. Yaginuma, Cell cycles in embryos of the silkworm, Bombyx mori: G_2-arrest at diapause stage. *Rouxs Arch. Dev. Biol.* **200**, 223–229 (1991).
8. O. Yamashita, Diapause hormone of the silkworm, *Bombyx mori*: Structure, gene expression and function. *J. Insect Physiol.* **42**, 669–679 (1996).
9. T. Homma *et al*., G protein-coupled receptor for diapause hormone, an inducer of *Bombyx* embryonic diapause. *Biochem. Biophys. Res. Commun.* **344**, 386–393 (2006).
10. A. Sato *et al*., Embryonic thermosensitive TRPA1 determines transgenerational diapause phenotype of the silkworm, *Bombyx mori*. *Proc. Natl. Acad. Sci. U.S.A.* **111**, E1249–E1255 (2014).
11. S. Fukuda, Function of the pupal brain and suboesophageal ganglion in the production of non-diapause and diapause eggs in the silkworm. *Annot. Zool. Jpn.* **25**, 149–155 (1952).
12. K. Matsutani, H. Sonobe, Control of diapause-factor secretion from the suboesophageal ganglion in the silkworm, *Bombyx mori*: The roles of the protocerebrum and tritocerebrum. *J. Insect Physiol.* **33**, 279–285 (1987).
13. A. Hagino, N. Kitagawa, K. Imai, O. Yamashita, K. Shiomi, Immunoreactive intensity of FXPRL amide neuropeptides in response to environmental conditions in the silkworm, *Bombyx mori*. *Cell Tissue Res.* **342**, 459–469 (2010).
14. T. Ichikawa, S. Aoki, I. Shimizu, Neuroendocrine control of diapause hormone secretion in the silkworm, *Bombyx mori*. *J. Insect Physiol.* **43**, 1101–1109 (1997).
15. A. Sedelnikova, B. E. Erkkila, H. Harris, S. O. Zakharkin, D. S. Weiss, Stoichiometry of a pore mutation that abolishes picrotoxin-mediated antagonism of the GABAA receptor. *J. Physiol.* **577**, 569–577 (2006).
16. S. Masiulis *et al*., $GABA_A$ receptor signalling mechanisms revealed by structural pharmacology. *Nature* **565**, 454–459 (2019).
17. I. Shimizu, T. Matsui, K. Hasegawa, Possible involvement of GABAergic neurons in regulation of diapause hormone secretion in the silkworm, *Bombyx mori*. *Zool. Sci.* **6**, 809–812 (1989).
18. S. D. Buckingham, P. C. Biggin, B. M. Sattelle, L. A. Brown, D. B. Sattelle, Insect GABA receptors: Splicing, editing, and targeting by antiparasitics and insecticides. *Mol. Pharmacol.* **68**, 942–951 (2005).
19. A. K. Jones, Genomics, cys-loop ligand-gated ion channels and new targets for the control of insect pests and vectors. *Curr. Opin. Insect Sci.* **30**, 1–7 (2018).
20. J. A. Veenstra, Isolation and structure of corazonin, a cardioactive peptide from the American cockroach. *FEBS Lett.* **250**, 231–234 (1989).
21. Y. Zhao, C. A. Bretz, S. A. Hawksworth, J. Hirsh, E. C. Johnson, Corazonin neurons function in sexually dimorphic circuitry that shape behavioral responses to stress in *Drosophila*. *PLoS One* **5**, e9141 (2010).
22. O. I. Kubrak, O. V. Lushchak, M. Zandawala, D. R. Nässel, Systemic corazonin signalling modulates stress responses and metabolism in *Drosophila*. *Open Biol.* **6**, 160152 (2016).
23. K. D. McClure, U. Heberlein, A small group of neurosecretory cells expressing the transcriptional regulator apontic and the neuropeptide corazonin mediate ethanol sedation in *Drosophila*. *J. Neurosci.* **33**, 4044–4054 (2013).
24. K. Sha *et al*., Regulation of ethanol-related behavior and ethanol metabolism by the Corazonin neurons and Corazonin receptor in *Drosophila melanogaster*. *PLoS One* **9**, e87062 (2014).
25. K. Varga *et al*., Loss of Atg16 delays the alcohol-induced sedation response via regulation of Corazonin neuropeptide production in *Drosophila*. *Sci. Rep.* **6**, 34641 (2016).

26. A. O. Bergland, H. S. Chae, Y. J. Kim, M. Tatar, Fine-scale mapping of natural variation in fly fecundity identifies neuronal domain of expression and function of an aquaporin. *PLoS Genet.* **8**, e1002631 (2012).
27. S. Tanaka, K. I. Harano, Y. Nishide, R. Sugahara, The mechanism controlling phenotypic plasticity of body color in the desert locust: Some recent progress. *Curr. Opin. Insect Sci.* **17**, 10–15 (2016).
28. Y. J. Kim *et al*., Corazonin receptor signaling in ecdysis initiation. *Proc. Natl. Acad. Sci. U.S.A.* **101**, 6704–6709 (2004).
29. E. Imura *et al*., The corazonin-PTTH neuronal axis controls systemic body growth by regulating basal ecdysteroid biosynthesis in Drosophila melanogaster. *Curr. Biol.* **30**, 2156–2165.e5 (2020).
30. J. Gospocic *et al*., The neuropeptide corazonin controls social behavior and caste identity in ants. *Cell* **170**, 748–759.e12 (2017).
31. F. Hauser, C. J. Grimmelikhuijzen, Evolution of the AKH/corazonin/ACP/GnRH receptor superfamily and their ligands in the Protostomia. *Gen. Comp. Endocrinol.* **209**, 35–49 (2014).
32. M. Zandawala, S. Tian, M. R. Elphick, The evolution and nomenclature of GnRH-type and corazonin-type neuropeptide signaling systems. *Gen. Comp. Endocrinol.* **264**, 64–77 (2018).
33. O. Yamashita, T. Yaginuma, "Silkworm eggs at low temperatures: Implication for sericulture" in *Insects at Low Temperature*, J. R. E. Lee, D. L. Denlinger, Eds. (Chapman and Hall, New York, 1991), pp. 424–445.
34. L. Roller, Y. Tanaka, S. Tanaka, Corazonin and corazonin-like substances in the central nervous system of the Pterygote and Apterygote insects. *Cell Tissue Res.* **312**, 393–406 (2003).
35. J. Yang *et al*., Specific activation of the G protein-coupled receptor BNGR-A21 by the neuropeptide corazonin from the silkworm, *Bombyx mori*, dually couples to the G(q) and G(s) signaling cascades. *J. Biol. Chem.* **288**, 11662–11675 (2013).
36. L. L. Yu, Y. J. Cui, G. J. Lang, M. Y. Zhang, C. X. Zhang, The ionotropic γ-aminobutyric acid receptor gene family of the silkworm, *Bombyx mori*. *Genome* **53**, 688–697 (2010).
37. Q. Wei, S. F. Wu, C. F. Gao, Molecular characterization and expression pattern of three GABA receptor-like subunits in the small brown planthopper *Laodelphax striatellus* (Hemiptera: Delphacidae). *Pestic. Biochem. Physiol.* **136**, 34–40 (2017).
38. Z. Q. Jia *et al*., Identification of the ionotropic GABA receptor-like subunits from the striped stem borer, Chilo suppressalis Walker (Lepidoptera: Pyralidae). *Pestic. Biochem. Physiol.* **155**, 36–44 (2019).
39. K. Schuske, A. A. Beg, E. M. Jorgensen, The GABA nervous system in *C. elegans*. *Trends Neurosci.* **27**, 407–414 (2004).
40. T. Ilg, M. Berger, S. Noack, A. Rohwer, M. Gaßel, Glutamate decarboxylase of the parasitic arthropods *Ctenocephalides felis* and *Rhipicephalus microplus*: Gene identification, cloning, expression, assay development, identification of inhibitors by high throughput screening and comparison with the orthologs from *Drosophila melanogaster* and mouse. *Insect Biochem. Mol. Biol.* **43**, 162–177 (2013).
41. N. Kapan, O. V. Lushchak, J. Luo, D. R. Nässel, Identified peptidergic neurons in the *Drosophila* brain regulate insulin-producing cells, stress responses and metabolism by coexpressed short neuropeptide F and corazonin. *Cell. Mol. Life Sci.* **69**, 4051–4066 (2012).
42. Y. J. Guh, T. K. Tamai, T. Yoshimura, The underlying mechanisms of vertebrate seasonal reproduction. *Proc. Jpn. Acad. Ser. B Phys. Biol. Sci.* **95**, 343–357 (2019).
43. C. J. Scott, J. L. Rose, A. J. Gunn, B. M. McGrath, Kisspeptin and the regulation of the reproductive axis in domestic animals. *J. Endocrinol.* **240**, R1–R16 (2018).
44. B. De Velasco, J. Shen, S. Go, V. Hartenstein, Embryonic development of the *Drosophila* corpus cardiacum, a neuroendocrine gland with similarity to the vertebrate pituitary, is controlled by sine oculis and glass. *Dev. Biol.* **274**, 280–294 (2004).
45. K. Shiomi *et al*., The Pitx homeobox gene in *Bombyx mori*: Regulation of DH-PBAN neuropeptide hormone gene expression. *Mol. Cell. Neurosci.* **34**, 209–218 (2007).
46. J. J. Tremblay, C. Lanctôt, J. Drouin, The pan-pituitary activator of transcription, Ptx1 (pituitary homeobox 1), acts in synergy with SF-1 and Pit1 and is an upstream regulator of the Lim-homeodomain gene Lim3/Lhx3. *Mol. Endocrinol.* **12**, 428–441 (1998).
47. Y. Tanaka, Y. Hua, L. Roller, S. Tanaka, Corazonin reduces the spinning rate in the silkworm, *Bombyx mori*. *J. Insect Physiol.* **48**, 707–714 (2002).
48. Y. Tanaka, J. Ishibashi, S. Tanaka, Comparison of structure-activity relations of corazonin using two different bioassay systems. *Peptides* **24**, 837–844 (2003).
49. Y. Shi *et al*., Identification and functional characterization of two orphan G-protein-coupled receptors for adipokinetic hormones from silkworm *Bombyx mori*. *J. Biol. Chem.* **286**, 42390–42402 (2011).
50. M. Watanabe, A. Fukuda, J. Nabekura, The role of GABA in the regulation of GnRH neurons. *Front. Neurosci.* **8**, 387 (2014).
51. L. Chen, K. A. Durkin, J. E. Casida, Structural model for gamma-aminobutyric acid receptor noncompetitive antagonist binding: Widely diverse structures fit the same site. *Proc. Natl. Acad. Sci. U.S.A.* **103**, 5185–5190 (2006).
52. M. Xu, D. F. Covey, M. H. Akabas, Interaction of picrotoxin with GABAA receptor channel-lining residues probed in cysteine mutants. *Biophys. J.* **69**, 1858–1867 (1995).
53. D. S. Wang, J. M. Mangin, G. Moonen, J. M. Rigo, P. Legendre, Mechanisms for picrotoxin block of alpha2 homomeric glycine receptors. *J. Biol. Chem.* **281**, 3841–3855 (2006).
54. C. Henry *et al*., Heterogeneous expression of GABA receptor-like subunits LCCH3 and GRD reveals functional diversity of GABA receptors in the honeybee *Apis mellifera*. *Br. J. Pharmacol.* **177**, 3924–3940 (2020).
55. G. Gisselmann, J. Plonka, H. Pusch, H. Hatt, Drosophila melanogaster GRD and LCCH3 subunits form heteromultimeric GABA-gated cation channels. *Br. J. Pharmacol.* **142**, 409–413 (2004).
56. A. Scimemi, Structure, function, and plasticity of GABA transporters. *Front. Cell. Neurosci.* **8**, 161 (2014).
57. D. Mbungu, L. S. Ross, S. S. Gill, Cloning, functional expression, and pharmacology of a GABA transporter from *Manduca sexta*. *Arch. Biochem. Biophys.* **318**, 489–497 (1995).
58. X. Gao, H. McLean, S. Caveney, C. Donly, Molecular cloning and functional characterization of a GABA transporter from the CNS of the cabbage looper, *Trichoplusia ni*. *Insect Biochem. Mol. Biol.* **29**, 609–623 (1999).
59. P. D. Gluckman, M. A. Hanson, H. G. Spencer, Predictive adaptive responses and human evolution. *Trends Ecol. Evol.* **20**, 527–533 (2005).
60. T. A. Mousseau, C. W. Fox, *Maternal Effects as Adaptations* (Oxford University Press, 1998).
61. Y. Takasu, T. Tamura, S. Sajwan, I. Kobayashi, M. Zurovec, The use of TALENs for nonhomologous end joining mutagenesis in silkworm and fruitfly. *Methods* **69**, 46–57 (2014).
62. N. Kitagawa *et al*., Establishment of a sandwich ELISA system to detect diapause hormone, and developmental profile of hormone levels in egg and subesophageal ganglion of the silkworm, Bombyx mori. *Zool. Sci.* **22**, 213–221 (2005).
63. K. Shiomi *et al*., Myocyte enhancer factor 2 (MEF2) is a key modulator of the expression of the prothoracicotropic hormone gene in the silkworm, Bombyx mori. *FEBS J.* **272**, 3853–3862 (2005).